J Fluoresc
DOI 10.1007/s10895-017-2051-0

ORIGINAL ARTICLE

Photophysics of Dihydroquinazolinone Derivatives: Experimental and Theoretical Studies

Mehboobali Pannipara[1] · **Abdullah G. Al-Sehemi**[1,2] · **Abul Kalam**[1,2] · **T. N. Mohammed Musthafa**[3]

Received: 5 October 2016 / Accepted: 19 February 2017

Abstract Herein, we report the synthesis of two dihydroquinazolinone derivative 2-(2-Hydroxy-naphthalen-1-yl)-2, 3-dihydro-1H-quinazolin-4-one (**1**) and 2-(3-Methyl-thiophen-2-yl)-2,3-dihydro-1H-quinazolin-4-one (**2**) by using 2-aminobenzamide, 2-hydroxybenzaldehyde and 3-methyl thiophene-2-carboxaldehyde. The synthesized compounds were characterized by 1H NMR, 13C NMR, FT-IR and its spectral, photophysical, intramolecular charge transfer characteristics were studied by absorption and emission spectroscopy. The synthesized compound exhibits significant changes in their photophysical properties depending on the solvent polarity. The observed bathochromic emission band and difference in Stokes shift on changing the polarity of the solvents clearly demonstrate the highly polar character of the excited state. The synthesized compounds were also studied by density functional theory (DFT) and time-dependent density functional theory (TDDFT) to expose the reproducibility by computational means.

Keywords Dihydroquinazolinone derivatives · Solvent effect · DFT studies

Introduction

Heterocyclic organic compounds containing atoms like Sulphur, Nitrogen and Oxygen are the most abundant and central skeletons that occur ubiquitously in a variety of synthetic drugs and bioactive products [1]. Among them, quinazoline and quinazolinone derivatives have attracted paramount attention owing to their widespread applications ranging from biomedical science to material science [2–6]. Though quinazolinones and their derivatives are endowed with diverse biological activities such as antitumour, antibiotic, anti-defibrillatory, antipyretic, analgesic, diuretic, antihistamine, antidepressant and vasodilating behavior [7–13], its photophysical phenomena are only minimally studied and are lesser known for their luminescent properties [14, 15]. Quinazolinone derivatives have attracted great interest for researchers around the world due to its distinctive photophysical properties such as intense luminescence, large Stokes shifts and significant photostability which can be tunable in response to the changes in pH and polarity of solvents [16].

The photophysical properties of pi-conjugated organic fluorophores containing donor-acceptor groups originate mainly from the intramolecular charge transfer state that depends mainly on the substituent effect and solvent properties [17]. Intramolecular charge transfer (ICT) in a molecule has a significant influence on the luminescence properties and is also required for nonlinear optical (NLO) processes. The quinazolinone ring which act as a π-deficient aromatic heterocycle having electron-withdrawing character, when incorporated with electron donating moiety can be used as push − pull structures for intramolecular charge transfer (ICT). Furthermore, upon incorporation of quinazolines in the backbone of pi- conjugated scaffolds, substantial reduction in the HOMO − LUMO energy band gap is observed [18, 19]. Since

✉ Abdullah G. Al-Sehemi
agmasq@gmail.com

[1] Research Center for Advanced Materials Science (RCAMS), King Khalid University, P.O. Box 9004, Abha 61413, Saudi Arabia

[2] Department of Chemistry, Faculty of Science, King Khalid University, P.O. Box 9004, Abha 61413, Saudi Arabia

[3] Department of Chemistry, MES Kalladi College, Mannarkkad, Kerala 678583, India

the nitrogen atoms of the quinazolinone rings are easily available for protonation, hydrogen bond formation and chelation, its derivatives have been exploited for the formation of supramolecular assemblies and sensors [20–23].

The absorption and emission properties of organic fluorophores that carry a charge centre depend on the physical properties of solvents such as polarity, polarizability and dielectric constant and hence, offer an insight to their excited state and thereby to access fundamental molecular properties [24]. Excitation of a molecule by a photon may leads to redistribution of electronic charges leading to conformational changes in the excited-state and hence changes in dipole moments. Knowledge of excited state electronic redistribution in a molecule is quite useful for designing future molecules that can be exploited in materials science research [25]. Though there exist many methods available in the literature for determination of dipole moments, the one with solvent effect (solvatochromic method); which is based on a linear correlation between the wavenumbers of the absorption and emission maxima and solvent polarity function is the simplest and the most widely accepted one as it is not equipment sensitive and not limited to small molecules [26].

In the current work, which is the continuation of our research in the area of synthesis and photophysical properties of organic molecules having donor–acceptor chromophores [27, 28], we report here, the synthesis of two dihydroquinazolinone derivative by reported protocol and explored their spectral and photophysical properties. The excited state properties of these compounds were further examined by applying DFT based calculation.

Experimental

Materials and Methods

All of the chemicals and solvents used in this study were of analytical grade and used without further purification. The reactions were monitored by TLC with the aid of UV light. 2-hydroxy-1-naphthaldehyde, 2-amino benzamide and 3-Methylthiophene 2- carboxaldehyde were purchased from Sigma–Aldrich and Merck. Stock solution of the compounds and its dilutions were prepared for UV–visible and fluorescent study at different concentrations.

Spectral Measurements

Gallenkamp melting point apparatus was used to determine the melting point and the infrared (IR) spectra were recorded on Shimadzu FT-IR 8400S infrared spectrophotometer using KBr pellets. The NMR (1H and 13C) spectra were recorded on a Bruker DPX-600 at 600 MHz and 150 MHz, respectively, using TMS as the internal standard. The chemical shift values are documented on δ scale and coupling constants (*J*) in Hertz; Splitting patterns were entitled as follows: s: singlet; d: doublet; m: multiplet. PG spectrophotometer was used to record the UV-Vis electronic absorption spectra, and the steady-state fluorescence spectra were measured using Varain Cary Eclipse spectrofluorophotometer using a rectangular quartz cell of dimensions 0.2 cm × 1 cm. The emission was monitored at right angle.The fluorescence quantum yield (ϕ_f) in different solvents were measured using a comparative method where quinine sulfate [12] was used as the reference and calculated using Eq. (1):

$$\phi_u = \phi_s \times \frac{I_u}{I_s} \times \frac{A_s}{A_u} \times \frac{n_u^2}{n_s^2} \tag{1}$$

where ϕ_u, ϕ_s are the fluorescence quantum yields of the unknown and standard, respectively,*I* denote the integrated emission intensity; A is the absorbance at excitation wavelength, and *n* denote the refractive index of the solvent. The subscript *u* and *s* stand for the unknown and standard, respectively.

Synthetic Procedure for 2-(2-Hydroxy-Naphthalen-1-Yl)-D-2, 3-Dihydro-1H-Quinazolin-4-One (1)

The title compound **1** was synthesized by a mixture of 2-amino benzamide(10 mmol), 2-hydroxy benzaldehyde (10 mmol) and sufanilic acid (1 mmol) in 50% aq ethanol (25 mL) at 70 °C and the progress of reaction was monitored by TLC. The obtained product was collected by simple filtration and washed several time with 50% aq. ethanol to get pure product as yellow solid. Melting point 164 °C; IR (KBr): 3150, 1669, 1492, 1417, 1360, 1153, 803, 707; ^{1}H NMR (600 MHz, CDCl$_3$) δ = 6.64–6.90 (dt, 1H, J = 0.8 and 7.8 Hz, Ar-H), 6.90 (dt, 1H, *J* = 0.8 and 7.8 Hz, Ar-H),6.68–6.70 (dd, 2H, *J* = 0.4 and 7.6 Hz, Ar-H), 7.05 (s, 1H, OH), 8.20 (s, 2H, NH), 5.35 (s, 1H), 7.22–7.26 (m, 1H, Ar-H), 7.34 (d, 1H, Ar-H), 7.48–7.50 (m, 4H, Ar-H), 7.60 (dd, 1H, *J* = 1.6 and 8.0 Hz, Ar-H); ^{13}C NMR (150 MHz, CDCl$_3$) δ = 82.4, 112.4, 114.9, 118.1, 126.8, 127.3, 125.6, 129.4136.3, 138.2, 136.3144.6, 147.8, 176.8.

Synthetic Procedure for 2-(3-Methyl-Thiophen-2-Yl) -2,3-Dihydro-1H-Quinazolin-4-One (2)

The title compound 2 was synthesized by a mixture of 2-amino benzamide (10 mmol), 3-Methylthiophene 2-carboxaldehyde (10 mmol) and sufanilic acid (1 mmol) in 50% aq. ethanol (25 mL) at 70^0 C and the progress of reaction

Scheme 1 Synthetic route of Compound **1** and **2**

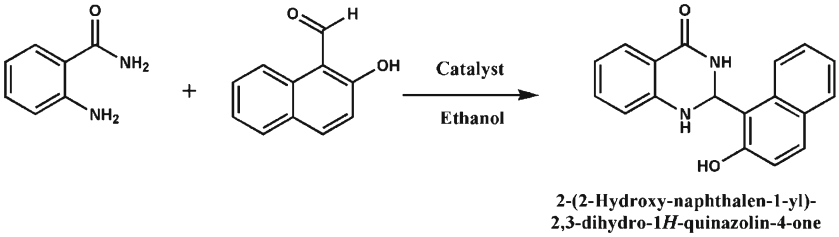

was monitored by TLC. The obtained product was collected by simple filtration and washed several time with 50% aq ethanol to get pure product as off-white solid. Melting point: 154-1560C; IR (KBr): 3027, 1640, 1542, 1417, 1360, 1153; 1H NMR (600 MHz, CDCl3) δ = 6.64–6.90 (dt, 1H, *J* = 0.8 and 7.8 Hz, Ar-H), 6.90 (dt, 1H, *J* = 0.8 and 7.8 Hz, Ar-H),6.68–6.70 (dd, 2H, *J* = 0.4 and 7.6 Hz, Ar-H), 5.16 (s, 1H), 8.02 (s, 2H, NH), 7.36–7.42 (m, 1H, Ar-H), 7.34 (dd, 1H, Ar-H), 7.68–7.50 (d, 1H, Ar-H), 2.60 (s, 3H); ^{13}C NMR (150 MHz, $CDCl_3$) δ = 32.6, 81.8, 116.4, 125.8, 126.3, 128.6, 129.4, 136.3, 138.2, 136.3144.6, 147.8, 178.6.

Results and Discussion

Chemistry

Two quinazolinone derivatives having intramolecular charge transfer characteristics, namely, 2-(2-Hydroxy-naphthalen-1-yl)- 2, 3-dihydro-1H-quinazolin-4-one (**1**) and 2-(3-Methyl-thiophen-2-yl)-2,3-dihydro-1H-quinazolin-4-one (**2**) have been synthesized and characterized. The structures of compounds were confirmed by IR, ^{1}H NMR and ^{13}C NMR. Schemes 1 and 2 outlines the synthetic route to the synthesis of two quinazolinone derivatives. Lippert–Mattaga and Reichardt's correlations were applied to calculate the change in dipole moments of the synthesized compounds. Solvents having different polarity have been used to investigate the solvent effect on theabsorption and emission spectra in detail.

Solvents Effect on Absorption and Emission Spectra

The electronic absorption spectra of compound **1**and **2**(~10^{-5} M) have been recorded in different solvents show only slight or negligible variation in the absorption spectra on changing the polarity of the solvents. Fig. 1 represents the absorption spectra of both synthesized compounds recorded in some selective solvents and the corresponding spectroscopic parameters in detail are collected in Tables 1 and 2. Compound **1** displays two structureless absorption band in the UV region (317–323 nm and 445–455 nm region) which are ascribed to $S_0 \rightarrow S_1$or $S_0 \rightarrow S_n$ transitions with molar absorption coefficients in the range of 16,100–24,200 M^{-1} cm^{-1} depending on the solvent whereas compound **2** exhibit only one absorption band at ~ 302–312 nm region with molar absorption coefficients in the range of 29,900–42,200 M^{-1}. The relatively high molar extinction coefficient in both compounds indicates that these could be π-π* type of transition as was found in other related compounds [29]. As inferred from Figs. 1 and 2, small blue shift is observed in absorption spectra due to greater degree of stabilization of the ground state in polar environments [30, 31]. This kind of blue shifted spectra has often reported in charge transfer systems due to the formation of hydrogen bonded solvated cluster between probe compounds and protic solvents.

The emission profile of both synthesized compounds shows dramatic change on increasing the solvent polarity from non polar to polar on exciting at 335 nm. As deciphered from Fig. 2, the emission spectrum of compound 1 undergo red shift of ~23 nm on going from polar aprotic solvents to polar protic solvents whereas the shift for compound 2 is 44 nm; suggesting the involvement of photo induced intramolecular charge transfer(ICT) state formation following photoexcitation. The emission spectral characteristics of compound **2** are predominated by emission from locally excited (LE) state in nonpolar hydrophobic solvents with one emission band. But increasing solvent polarity

Scheme 2 Synthetic route of Compound **1** and **2**

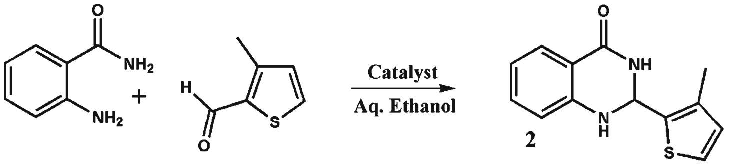

2-(3-Methyl-thiophen-2-yl)-2,3-dihydro-1*H*-quinazolin-4-one

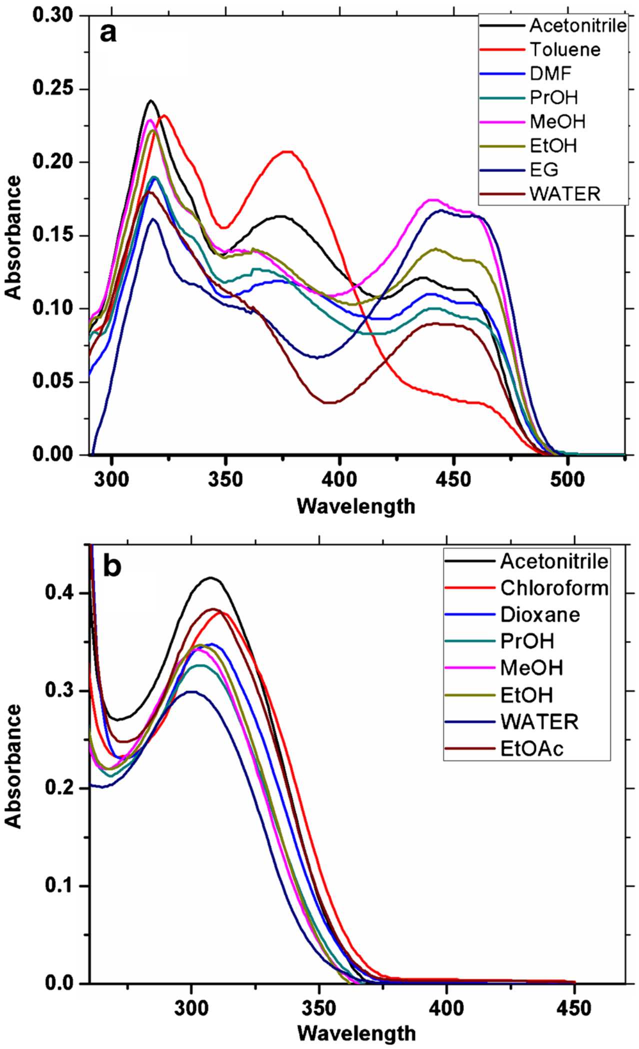

Fig. 1 Electronic absorption spectra of (1×10^{-5} M) compound **1** (*Panel A*) and **2** (*Panel B*)

results in a large red-shifted emission band in addition to the short wavelength band suggesting the involvement of photo induced intramolecular charge transfer (ICT) in the singlet excited state with larger dipole moment in the excited state [32]. Furthermore, apart from solvent polarity effect, hydrogen bonding effect of solvent also responsible for the red shift of the emission band, as we can see in case of acetonitrile and methanol where the solvent polarities are equal (expressed in Δf). Compound **2** shows a red shift of 26 nm in methanol (~435 nm) from that of the emission band in acetonitrile (~409 nm) which clearly illustrate the hydrogen bonding effect in this charge transfer system [28].

Estimation of Dipole Moment Using Solvatochromic Methods

Lippert- Mattaga and Reichardt's methods has been applied to calculate the difference in the dipole moment between the excited and ground state, Eq. (S1, S2, S3, S4, S5 and S6) (see Electronic supplementary information (ESI)) [33–36], which is based on the correlation of solvent orientation polarizability parameter (Δf) and dimensionless microscopic solvent polarity parameter (E_T^N) of solvents with energy difference between the ground and excited states (Stokes' shift). The calculated change in dipole moments ($\Delta\mu$) for compounds **1** and **2** using Lippert-Mattaga method, which is based on the slope of the linear plot between Stokes shift with Δf, were found to be 5.17 and 8.26 D (Fig. 3). Reichardt's method; which is based on the correlation of dimensionless microscopic solvent polarity parameter (E_T^N) with Stokes' shift, have reign over other method as it can include the polarizability of solute molecules apart from dipole-dipole interactions. The value for $\Delta\mu$obtained by this method from the slope of the linear plot between E_T^N

Table 1 Spectral and photophysical parameters of compound **1** in different solvents

Solvents	λ_{abs} (nm)	λ_{em}(nm)	$\Delta\bar{\nu}$ (cm^{-1})	ε M^{-1} cm^{-1}	*f*	μ$_{12}$ Debye	E$_T$(30) K cal mol^{-1}	*Δf(D,n)*	E_T^N
Acetonitrile	317	403	6732	24,200	0.90	7.78	45.6	0.304	0.472
Chloroform	321	413	6940	21,100	0.77	7.23	39.1	0.148	0.259
Dioxane	319	404	6595	21,700	0.80	7.37	36	0.021	0.164
Ethyl Acetate	319	402	6472	21,300	0.78	7.25	38.1	0.199	0.424
Toluene	323	407	6390	23,200	0.84	7.58	33.9	0.0132	0.0987
THF	320	402	6374	21,500	0.76	7.18	37.4	0.2096	0.21
DMF	320	407	6680	18,800	0.18	3.47	43.8	0.274	0.404
Propanol	319	424	7763	19,000	0.26	4.21	49.2	0.274	0.570
Methanol	317	416	7507	22,900	0.33	4.71	55.4	0.308	0.762
Ethanol	318	421	7694	22,000	0.24	3.99	51.9	0.288	0.654
EG	318	413	7233	16,100	0.50	5.83	49.2	0.274	0.79
Water	317	426	8072	17,900	0.36	4.90	63.1	0.263	1

Table 2 Spectral and photophysical parameters of compound **2** in different solvents

Solvents	λ_{abs} (nm)	λ_{em}(nm)	$\Delta\overline{\nu}$ (cm^{-1})	ε M^{-1} cm^{-1}	f	μ_{12} Debye	$E_T(30)$ K cal mol^{-1}	$\Delta f(D,n)$	E_T^N
Acetonitrile	307	409	8123	41,600	1.26	9.05	45.6	0.304	0.472
Chloroform	312	418	8128	38,000	1.02	8.22	39.1	0.148	0.259
Dioxane	308	400	7468	34,800	0.83	7.37	36	0.021	0.164
Ethyl Acetate	309	398	7237	38,400	1.04	8.24	38.1	0.199	0.424
Toluene	313	403	7135	37,000	1.01	8.18	33.9	0.0132	0.0987
THF	311	398	7029	36,400	0.77	7.10	37.4	0.2096	0.21
DMF	309	406	7732	42,200	1.24	9.02	43.8	0.274	0.404
Propanol	303	429	9693	32,600	0.91	7.65	49.2	0.274	0.570
Methanol	303	435	10,015	34,200	0.85	7.39	55.4	0.308	0.762
Ethanol	303	429	9693	34,700	0.95	7.83	51.9	0.288	0.654
Water	302	444	10,590	29,900	0.94	7.76	63.1	0.263	1

with Stokes' shift is found to be 2.01 and 3.11 D, respectively (Fig. 4).

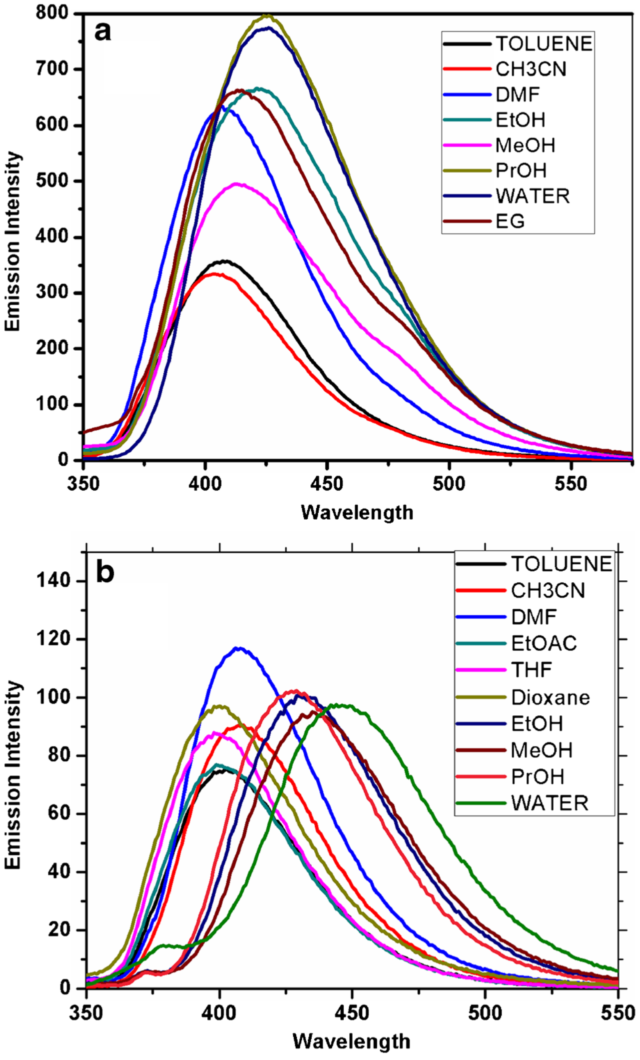

Fig. 2 Emission spectra of (1 × 10^{-5} M) compound **1** (Panel A) and **2** (Panel B)

The oscillator strength (f) and transition dipole moment (μ_{12}) of the molecules gives an insight into the charge transfer

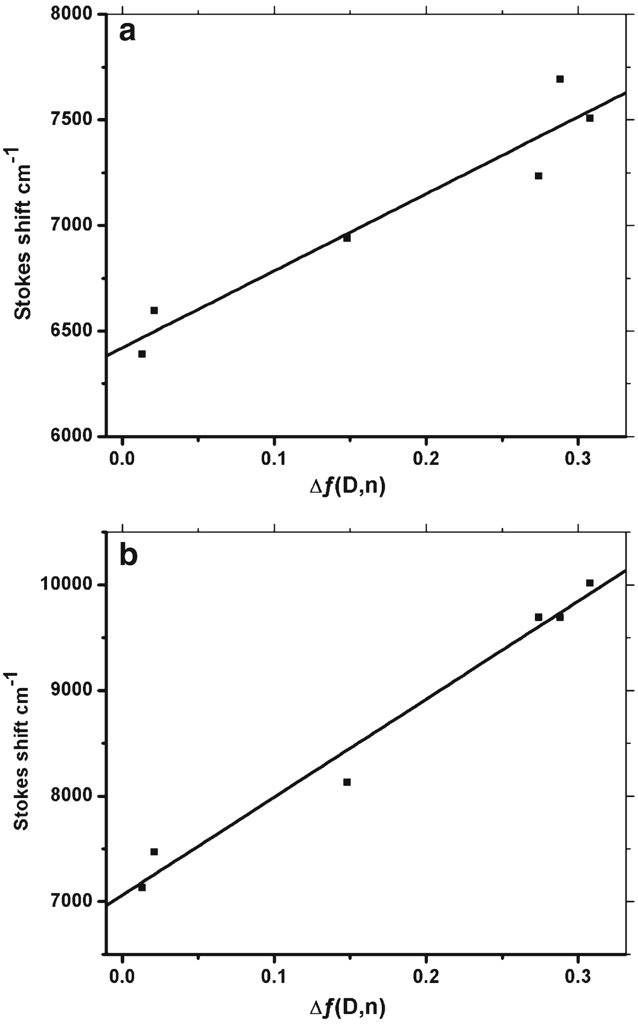

Fig. 3 Correlations of Stokes shift with the solvent polarity function ((Δf) for **1** (Panel A) and **2** (Panel B)

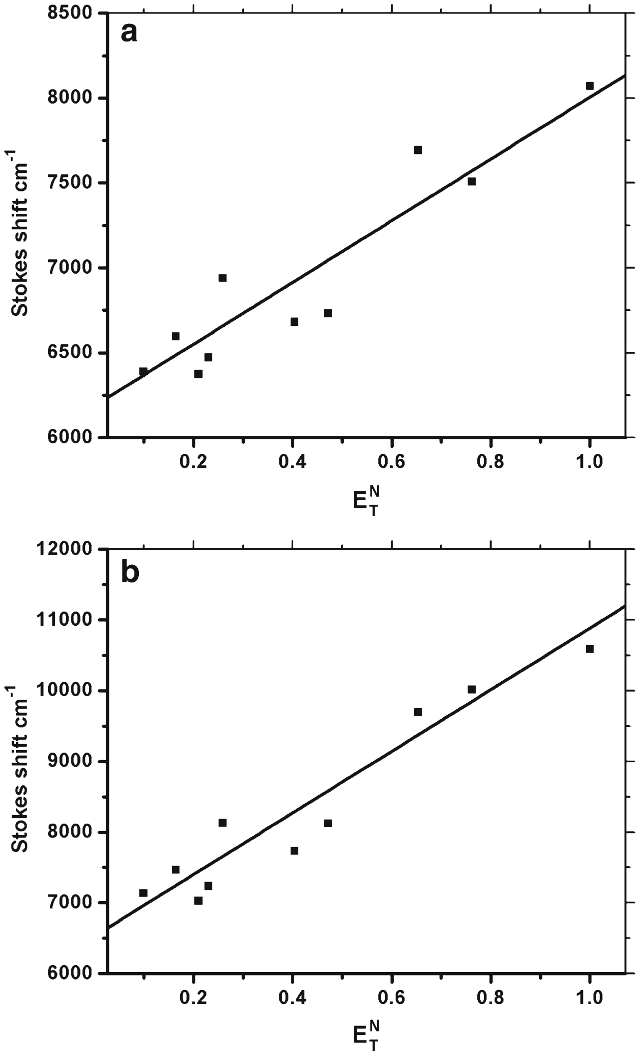

Fig. 4 Correlation of the Stokes' shift with E_T^N for compound **1** (Panel A) and **2** (Panel B)

character of the fluorophore where the oscillator strength values give a measure of the effective number of electronic transition from the ground to excited state by providing the absorption area in the electronic spectrum.

The experimental oscillator strength values were ascertained using Eq. (2) [37]

$$f = 4.32 \times 10^{-9} \int \varepsilon\left(\overline{\nu}\right)\, d\overline{\nu} \tag{2}$$

where, ε is the numerical value for molar decadic extinction coefficient measured in L mol^{-1} cm^{-1} and $\overline{\nu}$ is the numerical value of the wave number (cm^{-1}).

Transition dipole moments (μ_{12}) for absorption in various solvents which gives the probability of radiative transitions, was calculated using Eq. (3) [38]:

$$\mu_{12}{}^{2} = \frac{f}{4.72 \ \times 10^{-7} E_{\max}} \tag{3}$$

where, *f* is the oscillator strength which shows the number of electrons whose transition from ground to excited state gives the absorption area of the electronic spectrum and $E_{\max}$ is the energy maximum absorption in cm^{-1} and values for f and μ_{12} are listed in Tables 1 and 2.

Theoretical Studies

The ground and electronic excited states geometric optimizations of both compounds are performed using density functional theory (DFT) and time-dependent density functional theory (TDDFT) methods, respectively, with the Gaussian 09 package [39]. The DFT was treated according to Becke's three parameter gradient-corrected exchange potential and the Lee–Yang–Parrgradient-corrected correlation potential (B3LYP) [40–42], and all calculations were performed by using 6-31G⁄ basis set [29]. This model has been widely used for geometry optimization and the determination of electronic properties [43]. TDDFT has been used to investigate absorption spectra and has proved to be an efficient approach [44, 45]. The polarizable continuum model (PCM) [46, 47] was used for evaluating bulk solvent effects at all stages. The PCM-TDB3LYP/6-31G⁄ level of theory was used to compute the absorption spectra in different solvents. The labeling scheme is shown in Fig. 5.

We applied the DFT method to obtain the ground state geometrical and electronic structure in the gas phase (as a control) and in solvents. TD-DFT was used to investigate the excited state properties in the gas phase and solvents, together with the 6-31G(d). In general, S1–C9, S1–C10, C7–N1 and C7–N2 bond lengths increase from ground state to excited state for all solvents used and the difference value 0.032, 0.032, 0.035, 0.035, 0.0043, 0.0046, 0.0046 and 0.0043Aˇ respectively. On the other hand, O2–H14, N1–H5 andN2–H7, bond lengths shortened from ground to excited states, i.e., 0.015, 0.039, 0.015, 0.039, 0.026, 0.026, 0.014and 0.014A°, respectively. In the both compounds, the quinazolinone moiety are planar to other rings and have dihedral angles of N12–C7–C9–C10 and S1–C9–C7–N2, between 120 to 170.0 in both ground and excited states.

Figure 6 illustrates the frontier molecular orbital, highest occupied molecular orbitals (HOMO) and lowest unoccupied molecular orbitals (LUMO). The HOMO is π bonding while the LUMO is of antibonding character with π electrons distributed over the naphthalene and thiophene ring with charge transfer. The HOMO–LUMO energy gap of this compound was calculated at theB3LYP/6-31G⁄ level of theory, (Fig. 6). Orbital energy level analysis at the B3LYP/6-31G⁄ level and the resultant HOMO–LUMO energy gap (Egap) have been used as an indicator of kinetic stability of a molecule. A large HOMO–LUMO gap implies a high kinetic stability and low chemical reactivity, because it is energetically unfavorable to add electrons to a high-lying LUMO or to remove electrons from a low-lying HOMO. As shown in Fig. 6, the HOMO is delocalized over the quinazolinone moiety where as LUMOs

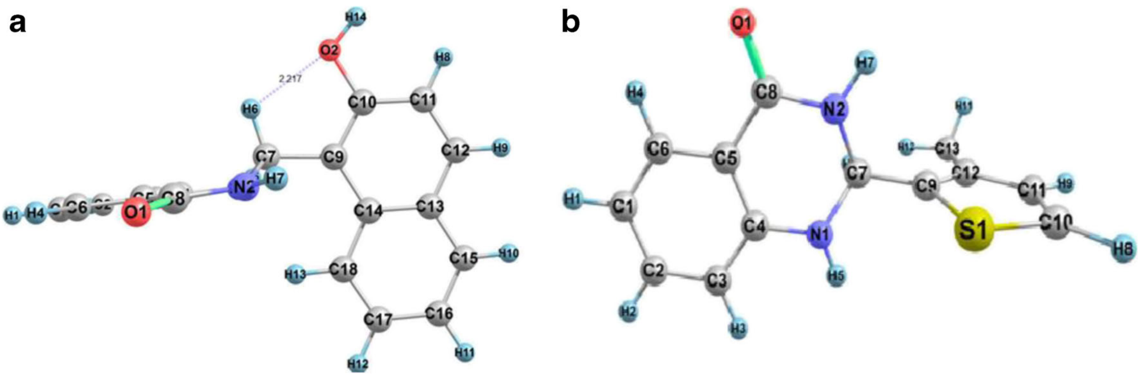

Fig. 5 Optimized molecular structure of compound **1** (Panel A) and **2** (Panel B)

are also distributed over the whole of the molecule. We also computed the HOMO–LUMO orbitals energy gap at the same level of theory in gas phase and found to be 4.36Ev for compound **1** and 4.83 eV for compound **2** respectively. The Experimental energy gap value of compound 1 in different solvents ranging from 3.4–3.7 eV whereas for compound 2 ranging from 3.5–3.65 eV respectively. The results revealed that the calculated energy gaps are not in bad agreement with the experimental values.

Conformational Analysis

The conformational analysis was carried out through the potential surface scan with B3LYP method using 6-31G** basis set in order to ascertain the most stable geometry of compound **1** and **2** (Fig. 7). During the scan, all the geometrical parameters were simultaneously relaxed while the dihedral angle N2-C7-C9-C10 is varied in steps of 10°ranging from − 180°to 180° for compound 1 and S1-C9-C7-N2 for compound **2**. The relative energies of less stable conformers with respect to the most stable form of compound **1** are 0.0 and 0.49 Kcal.mol^{-1} and 7.7 kcal mol^{-1} for the unstable rotamer. The energy difference between the most stable and other conformations of compound **2** is 3.5 kcal mol^{-1}.

For modeling and scanning calculation the initial guess of compound **1** and **2**, for the stable rotamers was first obtained from the optimization using B3LYP/6-31G(p, d) and transformed into the Z-matrix format with Babel program, the model starting geometry of R1 was obtained by driving procedure in Hyper Chem. To aid the future design of atropisomeric form of

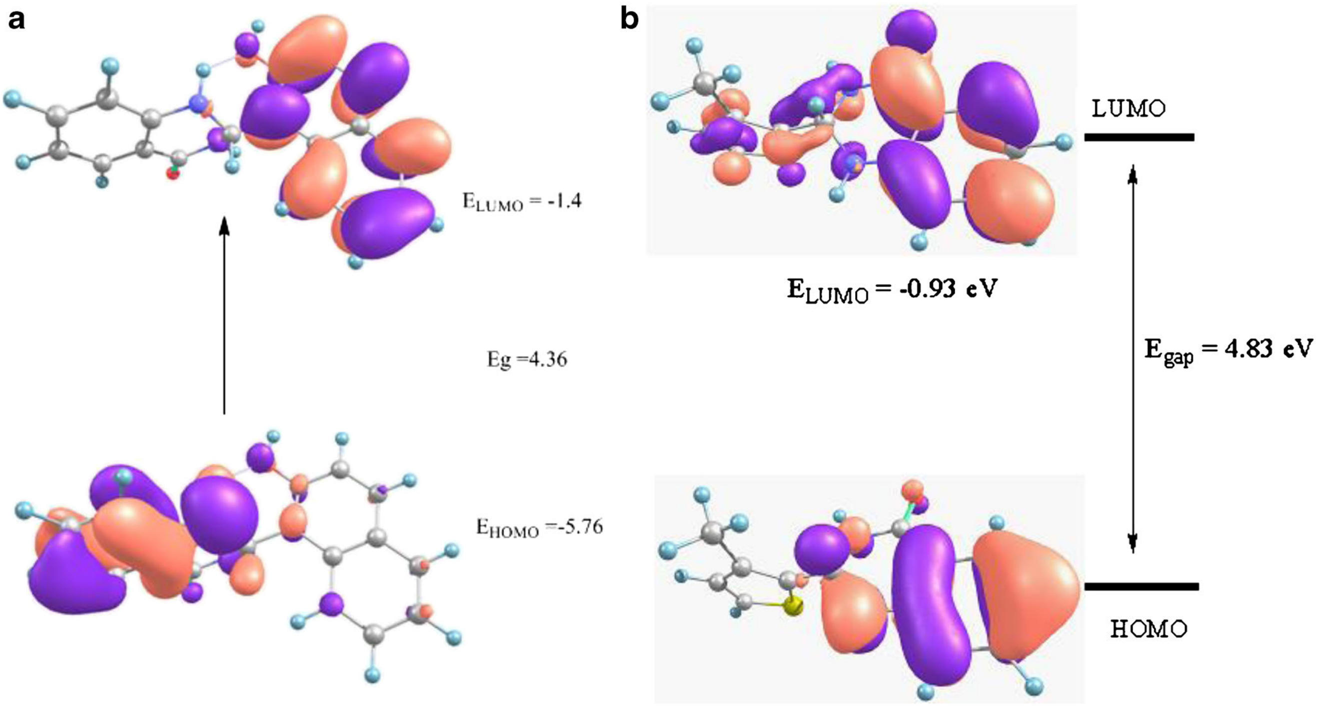

Fig. 6 The graphical presentation of the highest occupied and lowest unoccupied molecular orbitals of compound **1** and **2** at B3LYP/6-31G⁄ level of theory

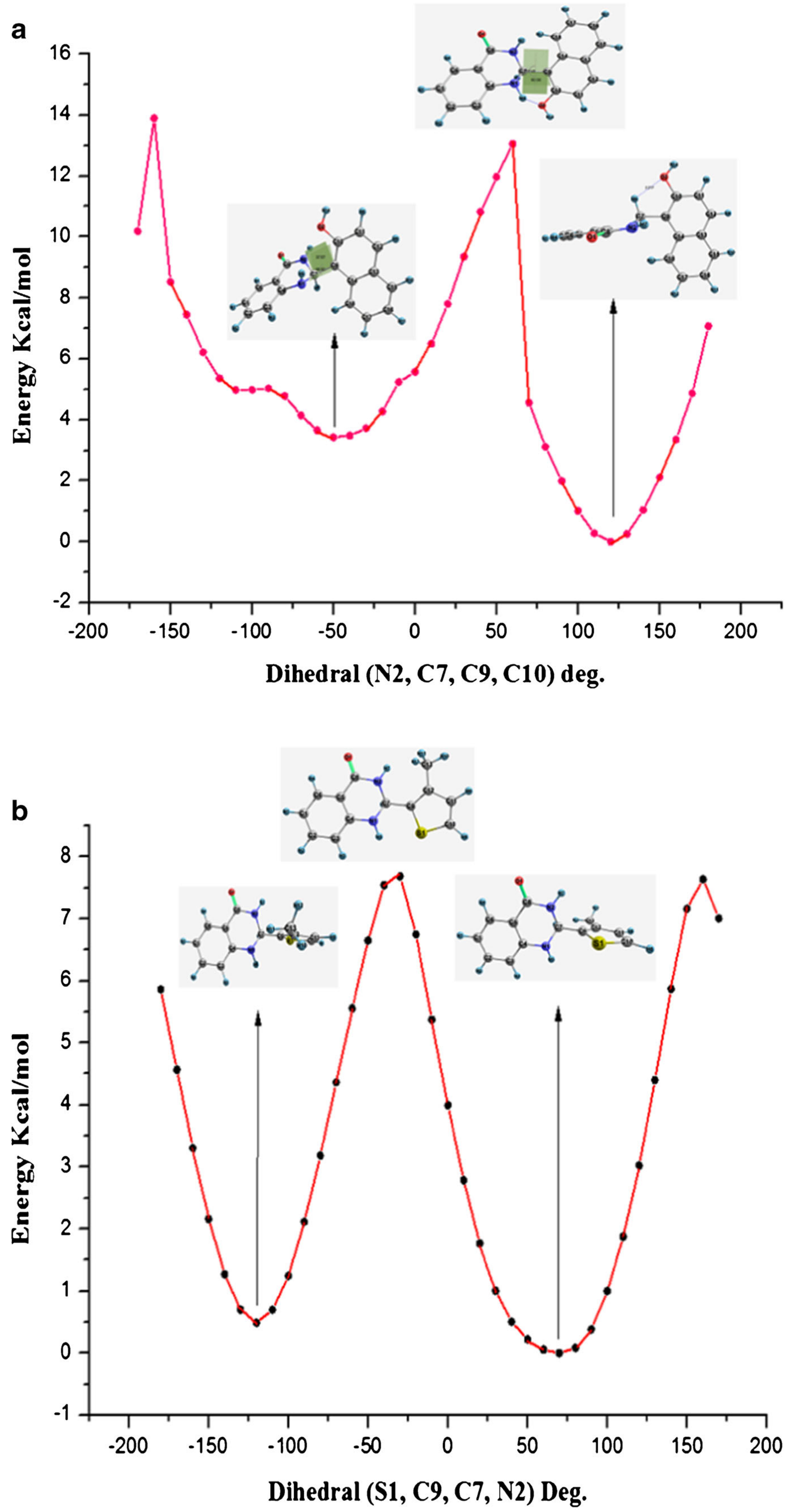

Fig. 7 The energy profile diagram of compounds **1** (Panel A) and **2** (Panel B)

compounds **1** and **2**, we set about to determining how well quantum chemical methods calculation could predict the rotation barriers around the C-C bonds on these compounds. To identify low energy conformations, the potential energy surface shape has been examined at the B3LYP/6-31G(p, d) levels. Potential energy surfaces of dihedral angle (N2-C7-C9-C10) for compound **1** and dihedral angle (S1-C9-C7-N2) for compound 2, from -180° to +180° in 10° steps, shown in Fig. 7. There are two minimum energy state found for the non-planar ground state of both compounds **1** and **2** together with two transition states. All levels of calculation of minimum structure and dihedral angle between quinazolinone rings and naphthalene ring for compound **1** and thiophene ring for **2** was found to be very close to (±70°) (Fig. 7). All calculations were performed for isolated molecules and solvents were not included. The maximum energy species obtained by these methods is not transition structures but the plot nonetheless provides a good approximation of the barrier to C-C bonds rotation. From the computational calculation, it appears that the OH group of naphthalene moiety more difficult to passes on front of the quinazolinone ring NH due to the hydrogen bond formed for **1** and due to clash of quinazolinone ring NH and methyl substituent of thiophene ring of **2**.

Conclusion

In summary, two dihydroquinazolinone derivatives having intramolecular charge characteristics have been synthesized and characterized by ^{1}H NMR, ^{13}C NMR and FT-IR. The spectral, photophysical and intramolecular charge transfer characteristics of these compounds were studied by absorption and emission spectroscopy. It is found that polarity and hydrogen bonding ability of the solvents play prominent effect on the absorption and emission spectra. The dual emission in polar solvents, polarity dependent red shifted emission band and large Stokes shift, support the occurrence of ICT in the excited state of the studied molecules. The density functional theory (DFT) was used to compute ground and excited state geometries of the molecule. The experimental results obtained are in good agreement with theoretical values.

References

1. Polshettiwar V, Varma RS (2007) Greener and sustainable approaches to thesynthesis of pharmaceutically active heterocycles. Curr Opin Drug Discov Dev 10:723–737
2. Marvania B, Lee PC, Chaniyara R, Dong HJ, Suman S, Kakadiya R, Chou TC, Lee TC, Shah A (2011) Design, synthesis and antitumor evaluation of phenyl N-mustard-quinazoline conjugates. Bioorg Med Chem 19:1987–1998
3. Shallal HM, Russu WA (2011) Discovery, synthesis, and investigation of the antitumor activity of novel piperazinylpyrimidine derivatives. Eur J Med Chem 46:2043–2057
4. Chilin A, Conconi MT, Marzaro G, Guiotto A, Urbani L, Tonus F, Parnigotto P (2010) Exploring epidermal growth factor receptor (EGFR) inhibitor features: the role of fused dioxygenated rings on the quinazoline scaffold. J Med Chem 53:1862–1866
5. Sagiv-Barfi I, Weiss E, Levitzki A (2010) Design, synthesis, and evaluation of quinazoline T cell proliferation inhibitors. Bioorg Med Chem 18:6404–6413
6. Sylvain A, Julian RL, Francoise RG (2014) Synthesis and photophysical studies of a series of quinazoline chromophores. J Organomet Chem 79:7564–7571
7. Alaimo RJ, Russel HE (1972) Antibacterial 2, 3-dihydro-2-(5-nitro-2-thienyl) quinazolin-4-(1H)-ones. J Med Chem 15:335–336
8. Levin JI, Venkatesan AM, Chan PS, Baker JS, Francisco G, Bailey T, Vice G, Katocs A, Lai F, Coupet J (1994) 2,3,6-substituted quinazolinones as angiotensin-ii receptor antagonists. Bioorg Med Chem Lett 4:1135–1140
9. Maskey RP, Shaaban M, Grun-Wollny I, Laatsch HJ (2004) Quinazolin-4-one derivatives from *Streptomyces* isolates. Nat Protoc 67:1131–1134
10. Pandey VK, Tusi S, Tusi Z, Raghubir R, Dixit M, Joshi MN, Bajpai SK (2004) Thiadiazolyl quinazolones as potential antiviral and antihypertensive agents. Indian J Chem 43B:180–183
11. Conolly DJ, Cusack D, O'Sullivan TP, Guiry PJ (2005) Synthesis of quinazolinones and quinazolines. Tetrahedron 61:10153–10202
12. Giovanni M, Ignazio C, Giulia S, Giorgio P, Martina DV, Adriana C, Paola B (2016) Substituted quinazolinones as kinase inhibitors endowed with anti-fibrotic properties. Eur J Med Chem 115:416–425
13. Mhaske SB, Argade NP (2006) The chemistry of recently isolated naturally occurring quinazolinone alkaloids. Tetrahedron 62:9787–9826
14. Cabrera-Rivera FA, Escalante J, Morales-Rojas H, Zigler DF, Schmidt RD, Jarocha LE, Forbes MD (2014) Journal of Photochemistry and Photobiology A: Chemistry 294:31–37.
15. Xiao-Bing Z, Guo C, Wei-Jun Z, Guo-Li S, Ru-Qin Y (2007) A fluorescent chemical sensor for Fe3+ based on blocking of intramolecular proton transfer of a quinazolinone derivative. Talanta 71: 171–177
16. Achelle S, Rodrıǵuez-Lopez J, Robin-le Guen F (2014) Synthesis and photophysical studies of a series of quinazoline chromophores. J Organomet Chem 79:7564–7571
17. Asiri AM, Alamry KA, Pannipara M, Al-Sehemi AG, El-Daly SA (2015) Spectroscopic investigation, photophysical parameters and DFT calculations of 4,40 (1E,10E)-2,20-(pyrazine-2,5-diyl) bis(ethene-2,1- diyl)bis(N,N-dimethylaniline) (PENDA) in different solvents. Spectrochim Acta A Mol Biomol Spectrosc 149: 722–730
18. Su SJ, Caib C, Kido J (2012) Three-carbazole-armed host materials with various cores for RGB phosphorescent organic light-emitting diodes. J Mater Chem 22:3447–3456
19. Wong KT, Hsu CC (2001) Control of the arrangement of dipolar orientation of pyrimidine inside the conjugated backbone. Org Lett 3:173–175
20. Petitjean A, Cuccia LA, Lehn JM, Nierengarten H, Schmutz M (2002) Cation-promoted hierarchical formation of supramolecular assemblies of self-organized helical molecular components. Angew Chem Int Ed 41:1195–1198
21. Hadad C, Achelle S, López-Solera I, García-Martínez JC, Rodríguez-López J (2013) Metal cation complexation studies of 4-arylvinyl-2,6-di(pyridin-2-yl) pyrimidines: effect on the optical properties. Dyes Pigments 97:230–237
22. Aranda AI, Achelle S, Hammerer F, Mahuteau-Betzer F, Teulade-Fichou MP (2012) Vinyl-diazine triphenylamines and their N-

methylated derivatives: synthesis, photophysical properties and application for staining DNA. Dyes Pigments 95:400–407

23. Robert MC, Stephen M (1985) Cyclisation of Schiff bases containing amide or hydroxamic acid groups to 1,2-dihydroquinazolin-4-ones; thermal decomposition reactions of the 1,2-dihydroquinazolin-4-ones. J Chem Soc Perkin Trans 1:2779–2783
24. Pithan PM, Decker D, Sardo MS, Viola G, Ihmels H (2016) Synthesis and fluorosolvatochromism of 3-arylnaphtho[1,2-b]quinolizinium derivatives. Beilstein J Org Chem 12:854–862
25. Valeur B, Berberan-Santos MN (2012) Molecular fluorescence. Principles and applications, 2nd edn. Wiley-VCH, Weinheim
26. Jayabharathi J, Kalaiarasi V, Thanikachalam V, Jayamoorthy K (2014) Estimation of excited state Dipolemoments from solvatochromic shifts–effect of Ph. J Fluoresc 24:599–612
27. Al-Sehemi AG, Pannipara M, Kalam A (2017) Quinazolinone derivative: Model compound for determination of dipole moment, solvatochromism and metal ion sensing. Spectrochim Acta A 171: 97–103
28. Pannipara M, Asiri AM, Alamry KA, Arshad MN, El-Daly SA (2015) Synthesis, spectral behaviour and photophysics of donor–acceptor kind of chalcones: excited state intramolecular charge transfer and fluorescence quenching studies. Spectrochim Acta A Mol Biomol Spectrosc 136:1893–1902
29. Chowdhury P, Panja S, Chakravorti S (2003) Excited state prototropic activities in 2-hydroxy 1-naphthaldehyde. J Phys Chem A 107:83–90
30. Lippert E, Luder W, Boos H (1962) In: Mangini A (ed) Advances in molecular spectroscopy. Pergamon Press, Oxford, p 443
31. Paul BK, Samanta A, Kar S, Guchhait N (2010) Evidence for excited state intramolecular charge transfer reaction in donor–acceptor molecule 5-(4-dimethylamino-phenyl)-penta-2,4-dienoic acid methyl ester: experimental and quantum chemical approach. J Lumin 130:1258–1267
32. Ziołek M, Filipczak K, Maciejewski A (2008) Spectroscopic and photophysical properties of salicylaldehyde azine (SAA) as a photochromic Schiff base suitable for heterogeneous studies. Chem Phys Lett 464:181–186
33. Lippert E (1957) Spectroscopic determination of the dipole moment of aromatic compounds in the first excited singlet state. Z Elektrochem 61:962–975
34. Mataga N, Kubota T (1970) Molecular interactions and electronic spectra. Marcel Dekker, Inc., New York
35. Ravi M, Soujanya T, Samanta A, Radhakrishnan TP (1995) Excitedstate dipole moments of some coumarin dyes from a solvatochromic method using the solvent polarity parameter E_T^N. J Chem Soc Faraday Trans 91(17):2739–2742
36. Reichardt C (1994) Solvatochromic dyes as solvent polarity indicators. Chem Rev 94(8):2319–2358
37. Coe BJ, Harris JA, Asselberghs I, Clays K, Olbrechts G, Persoons A, Hupp JT, Johnson RC, Coles SJ, Hursthouse MB, Nakatani K (2002) Quadratic nonlinear optical properties of N-aryl stilbazolium dyes. Adv Funct Mater 12:110–116
38. Gordon P, Gregory P (1987) Organic chemistry in colour. Chimia, Moskva
39. Frisch MJ, Trucks GW, Schlegel HB, Scuseria GE, Robb MA, Cheeseman JR, Scalmani G, Barone V, Mennucci B, Petersson GA, Nakatsuji H, Caricato M, Li X, Hratchian HP, Izmaylov AF, Bloino J, Zheng G, Sonnenberg JL, Hada M, Ehara M, Toyota K, Fukuda R, Hasegawa J, Ishida M, Nakajima T, Honda Y, Kitao O, Nakai H, Vreven T, Montgomery JA, Peralta JE, Ogliaro F, Bearpark M, Heyd JJ, Brothers E, Kudin KN, Staroverov VN, Kobayashi R, Normand J, Raghavachari K, Rendell A, Burant JC, Iyengar SS, Tomasi J, Cossi M, Rega N, Millam JM, Klene M, Knox JE, Cross JB, Bakken V, Adamo C, Jaramillo J, Gomperts R, Stratmann RE, Yazyev O, Austin AJ, Cammi R, Pomelli C, Ochterski JW, Martin RL, Morokuma K, Zakrzewski VG, Voth GA, Salvador P, Dannenberg JJ, Dapprich S, Daniels AD, Farkas O, Foresman JB, Ortiz JV, Cioslowski J, Fox DJ (2009) Gaussian 09, Revision A.1. Gaussian Inc, Wallingford
40. Becke AD (1993) Density-functional thermochemistry. III The role of exact exchange. J Chem Phys 98(7):5648–5652
41. Miehlich B, Savin A, Stoll H, Preuss H (1989) Results obtained with the correlation energy density functionals of becke and Lee, Yang and Parr. Chem Phys Lett 157:200–206
42. Lee C, Yang W, Parr RG (1988) Development of the Colle-Salvetti correlation-energy formula into a functional of the electron density. Phys Rev B 37:785–789
43. Sun J, Song J, Zhao Y, Liang WZ (2007) Real-time propagation of the reduced one-electron density matrix in atom-centered Gaussian orbitals: Application to absorption spectra of silicon clusters. J Chem Phys 127:234,107
44. El-Daly SA, Asiri AM, Alamry KA, Al-Sehemi AG (2013) Photophysical properties, photostability and laser activity of 2,6-bis [β-(2-benzoxazolyl) vinyl] naphthalene (BBVN). J Mol Struct 1037:323–331
45. Zhang CR, Liang WZ, Chen HS, Chen YH, Wei ZQ, Wu YZ (2008) Theoretical studies on the geometrical and electronic structures of N-methyle-3,4-fulleropyrrolidine. J Mol Struct (THEOCHEM) 862(2008):98–104
46. Matthews D, Infelta P, Grätzel M (1996) Calculation of the photocurrent– potential characteristic for regenerative, sensitized semiconductor electrodes. Sol Energy Mater Sol Cells 44:119–155
47. Cossi M, Barone V (2001) Time-dependent density functional theory for molecules in liquid solutions. J Chem Phys 115:4708–4717